Valence photoionization of the N_2 molecule in the region of the N $1s \rightarrow$ Rydberg excitations

A. Kivimäki,[1,*] R. Sankari,[2] R. Flammini,[3] M. Coreno,[3] J. Álvarez-Ruiz,[4] and R. Richter[5]

[1]*Consiglio Nazionale delle Ricerche, Istituto Officina dei Materiali, Laboratorio Nazionale Tecnologie Avanzate e Nanoscienza, 34149 Trieste, Italy*

[2]*MAX IV Laboratory, University of Lund, Box 118, 22100 Lund, Sweden*

[3]*Consiglio Nazionale delle Ricerche, Istituto di Metodologie Inorganiche e dei Plasmi, Via Salaria km 29.300, 00019 Monterotondo Scalo, Rome, Italy*

[4]*Instituto de Fusión Nuclear, Universidad Politécnica de Madrid, José Gutiérrez Abascal 2, 28006 Madrid, Spain*

[5]*Sincrotrone Trieste, Area Science Park, 34149 Trieste, Italy*

(Received 26 April 2012; revised manuscript received 12 June 2012; published 31 July 2012)

The intensities of the X and A valence photoelectron lines of N_2 have been found to display Fano line shapes as a function of photon energy around the N $1s \rightarrow$ Rydberg excitations. The vibrational intensity distributions of these photoelectron lines change at the N $1s \rightarrow 3s\sigma$ and $3p\pi$ resonances. These effects indicate interference between direct and resonant photoionization channels. Our numerical simulations reproduce quite well the experimental results.

DOI: 10.1103/PhysRevA.86.012516 PACS number(s): 33.60.+q, 33.80.Eh

I. INTRODUCTION

The N_2 molecule is a prototypical case to study electronic decay from core-excited states in molecules. These studies have concentrated on the N $1s \rightarrow 1\pi_g(\pi^*)$ excitation and its subsequent decay by electron emission, known as resonant Auger decay (see, e.g., Refs. [1–5]). Resonant Auger decay is the predominant decay channel of core-excited states in N_2 and consequently the main contributor (of the order of 99%) to the lifetime widths of the corresponding absorption features, which are slightly above 100 meV [6]. A subset of resonant Auger transitions, participator transitions, populates the same one-hole ($1h$) final states as direct valence photoionization, which greatly modifies the vibrational structure of the valence photoelectron lines. The changes can be understood in the framework of lifetime vibrational interference (LVI) theory and can be readily simulated if the vibrational functions are available (see, e.g., Refs. [2,5]).

The physical meaning of the LVI phenomenom can be desribed as follows. A transition from the molecular ground state to a core-excited state can induce the excitation of vibrational modes. If the vibrational energy ω_e and the lifetime width of the core-excited state are of similar magnitude (ω_e is usually around 300 meV for N_2 and N_2^+ [7]) it is possible to excite coherently different vibrational states using any photon energy close to the resonant energy. Then the participator intensity to a given vibrational level of the final ionic state ($1h$ state) is determined by the exact superposition of the vibrational levels in the core-excited state and can vary greatly when the photon energy is changed. The LVI theory assumes that only resonant channels are important for the intensity of the final state and direct photoionization can be neglected. Carravetta *et al.* [8] presented model calculations on participator decay of the CO molecule at the C $1s \rightarrow \pi^*$ excitation with and without direct photoionization. They showed that the experimental branching ratios of the photoelectron lines across the resonance, which are asymmetric, can only be reproduced when direct photoionization and its interference with resonant channels are included. Tanaka *et al.* [9] later carried out numerical simulations under such conditions for the vibrational intensities of the X and A valence photoelectron bands of the CO molecule at the O $1s \rightarrow \pi^*$ excitation.

Resonant Auger decay from core-to-Rydberg excited states of N_2 has been studied surprisingly little. The complete decay spectra taken at the two first Rydberg excitations, N $1s \rightarrow 3s\sigma$ and $3p\pi$, have been reported by Eberhardt *et al.* [10] and Shigemasa *et al.* [11]. It is generally considered that participator decay is not an important decay channel from core-to-Rydberg excited states because diffuse Rydberg orbitals have very small overlap with the core hole. Kugeler *et al.* [12] determined the photoionization cross sections of the outer-valence photoelectron lines, i.e., of the $3\sigma_g^{-1}$ X, $1\pi_u^{-1}$ A, and $2\sigma_u^{-1}$ B states of N_2^+, in a wide photon energy region across the N $1s$ edge, including few energies that corresponded to core-to-Rydberg excitations. They observed that the partial photoionization cross sections exhibit clear deviations from the asymptotic behavior at these energies, which hints that participator decay does play a role in the decay of core-to-Rydberg excited states.

In the present work, we study valence photoionization of the N_2 molecule at the N $1s \rightarrow$ Rydberg excitations. This is found to be a case where direct and resonant ionization channels are of similar importance.

II. EXPERIMENT

The experiments were performed at the Gas Phase Photoemission beamline at the Elettra synchrotron radiation laboratory in Trieste, Italy. The beamline has been described before [13]. A commercial hemispherical electron analyzer (VG i220) was used to analyze the kinetic energies of the emitted electrons. It was mounted at the so-called magic angle in the dipole plane, ensuring that the intensity distributions observed are equal to the angle-integrated ones. The kinetic energy resolution of about 140 meV was used at selected photon energies to resolve the vibrational structure of the

*Corresponding author; kivimaki@iom.cnr.it

valence photoelectron lines. A series of photoelectron spectra was measured across the N $1s \rightarrow$ Rydberg excitations with 0.4-eV kinetic energy resolution, which was sufficient to obtain the integrated intensities of the X, A, and B photoelectron bands. The photon energy resolution was about 120 meV in all these measurements.

III. NUMERICAL SIMULATIONS

Tanaka *et al.* [9] considered a situation where both direct and resonant photoionization channels are important for the intensity distribution of vibrational lines in the photoelectron spectrum. Using their notations, the intensity of the vibrational component f of the final ionic state at the excitation energy ω can be calculated as

$$I_f(\omega) = |D\langle f|0\rangle|^2 + I_f^{\mathrm{LVI}}(\omega) + \sum_n \frac{2DM(\omega-\omega_{n0})\langle f|0\rangle\langle f|n\rangle\langle n|0\rangle}{(\omega-\omega_{n0})^2+\frac{\Gamma^2}{4}}, \quad (1)$$

where the first term stands for direct photoionization, the second term denotes lifetime vibrational interference over the resonant channels, and the third term represents interference between the direct and resonant channels. Here M is the electronic transition moment for the resonant Auger transition in question; $|0\rangle$, $|n\rangle$, and $|f\rangle$ denote the vibrational wave functions of the ground, core-excited, and final states, respectively; Γ is the lifetime width of the core-excited state; and ω_{n0} is the energy of the core-excited vibrational state $|n\rangle$ with respect to the ground state $|0\rangle$. The explicit form of the LVI term can be found in Ref. [9]. We have written a procedure for the data analysis program IGOR PRO [14] that calculates the resulting intensity distribution with M and D as input parameters, when the overlaps of the vibrational wave functions are provided. The Franck-Condon factors and overlap integrals needed in the analysis were calculated using a modified version of the CONFRON program [15].

IV. RESULTS AND DISCUSSION

Figure 1 shows three outer-valence photoelectron spectra measured with vibrational resolution. The spectra have been approximately scaled so that the most intense peak ($B,\upsilon' = 0$ state) has the same height. The lowermost spectrum was measured at a photon energy of 385 eV, which is well below all the N $1s$ excitations, and it represents the contribution of direct photoionization only. When photon energy was tuned to the N $1s \rightarrow 3s\sigma,\upsilon = 0$ and N $1s \rightarrow 3p\pi,\upsilon = 0$ resonances (middle and top spectra, respectively), the biggest changes occurred in the A state: Its intensity increased relative to the X and B states and the vibrational levels up to $\upsilon' = 6$ or 7 became visible. The relative intensities of the vibrational levels $\upsilon' = 0,1$ of the X state also increase slightly at the N $1s \rightarrow 3s\sigma$ and N $1s \rightarrow 3p\pi$ resonances and the $\upsilon' = 2$ level becomes weakly populated. An obvious reason for all these changes is that participator decay contributes to the valence photoelectron spectrum at the N $1s \rightarrow 3s\sigma$ and $3p\pi$ Rydberg excitations.

In the simulations of the photoelectron spectra, the potential energy curves of the ground state, core-excited state, and final ionic state were described by Morse potentials. The spectroscopic constants of the molecular ground state and the three lowest states of the molecular ion are well known [7]. For the core-to-Rydberg excited states, we have used the transition energies from Ref. [16] as well as the internuclear distances R_e and the vibrational energies ω_e from Ref. [17]. The anharmonic corrections $\omega_e\chi_e$ were not given for the core-to-Rydberg excited states in Ref. [17] and we have assumed them to be the same as for the molecular ground state. This assumption should have no noticeable effects on our results. The lifetime broadenings Γ of 113±5 and 107±5 meV have been reported for the N $1s^{-1}3s\sigma^1,\upsilon = 0$ and N $1s^{-1}3p\pi^1,\upsilon = 0$ states, respectively [6], and these values were used in the simulations.

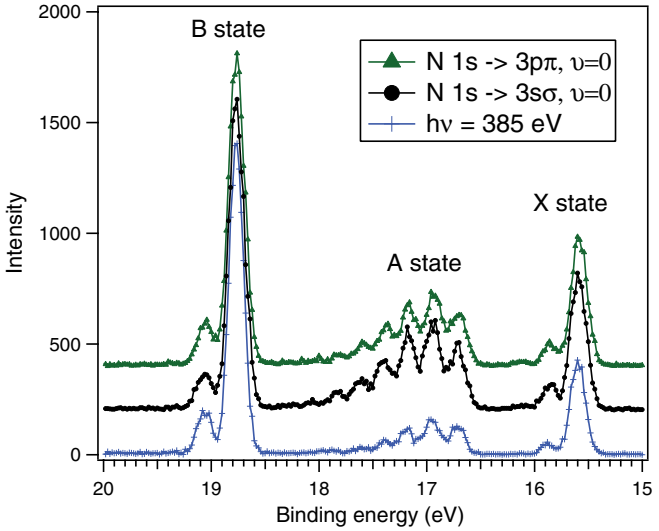

FIG. 1. (Color online) Valence photoelectron spectrum of N_2 measured at a photon energy of 385 eV (bottom), at the N $1s \rightarrow 3s\sigma,\upsilon = 0$ resonance (middle), and at the N $1s \rightarrow 3p\pi,\upsilon = 0$ resonance (top). The baselines are shifted for clarity; the background levels are essentially zero.

As an example, we show in Fig. 2 the simulation results for the $1\pi_u^{-1}$ A state at the N $1s \rightarrow 3p\pi,\upsilon = 0$ and $\upsilon = 1$ resonances. The best correspondence with the experiment was found with a D:M ratio equal to 23(±1). Figures 2(b) and 2(d) give the simulated partial intensity curves for different contributions. Direct photoionization is predicted to be dominant at both excitations. In the $\upsilon = 0$ spectrum, LVI enhances the intensities of all the vibrational levels, but particularly of those with $\upsilon' \geqslant 2$. The effect of interference between resonant and direct photoionization mostly manifests itself so as to cancel some of the intensity increase due to LVI for the vibrational levels $\upsilon' = 0$ and 1. In the $\upsilon = 1$ spectrum, the effect of LVI is much weaker, while the interference between direct and resonant photoionization has become more important than at the N $1s \rightarrow 3p\pi,\upsilon = 0$ excitation. Furthermore, it is mostly constructive, increasing the intensities of the vibrational levels $\upsilon' > 0$. These simulations should be considered qualitative only. An obvious inadequacy is that we have neglected the contribution of the weak N $1s \rightarrow 3p\sigma$ excitation, which occurs between the N $1s \rightarrow 3p\pi,\upsilon = 0$ and $\upsilon = 1$ excitations [16].

The photoelectron spectrum of N_2 was measured with a kinetic energy resolution of 0.4 eV in the photon energy region that covers the N $1s \rightarrow$ Rydberg excitations. The intensities

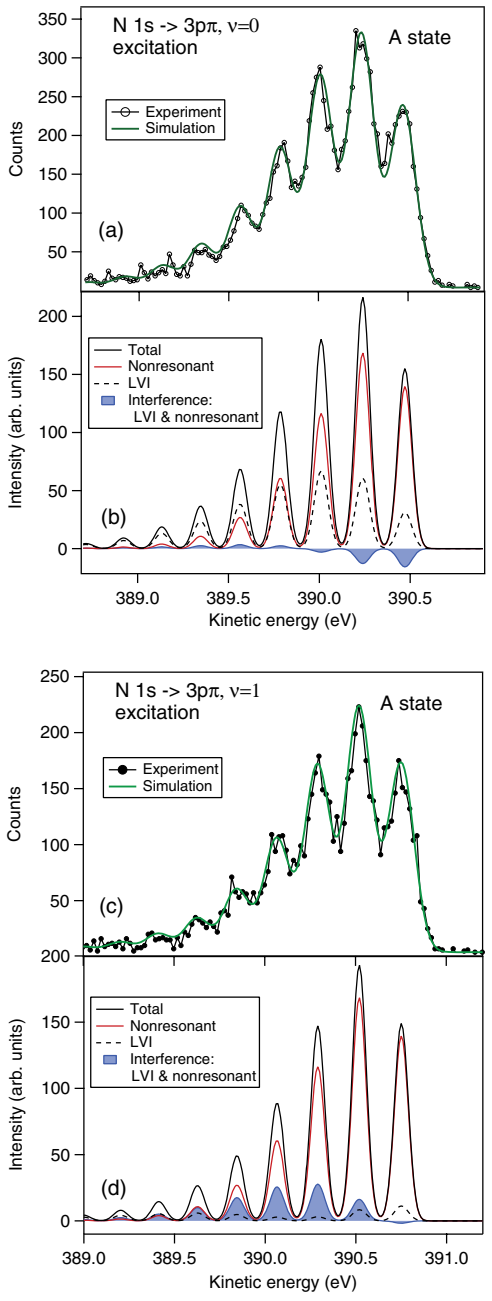

FIG. 2. (Color online) Photoelectron spectrum of N_2 in the region of the $1\pi_u^{-1} A$ state, measured at the N $1s \rightarrow 3p\pi, \upsilon = 0$ (a) and $\upsilon = 1$ (c) resonances, respectively. The thick green curves display the final results of simulation. (b) and (d) The different partial contributions to the simulated intensity are shown separately before convolution with the electron analyzer broadening.

of the X, A, and B states were determined by integrating the counts over the peaks and are shown in Fig. 3. Those of the X and A states are clearly affected by all the most intense Rydberg excitations. The effects on the B state are more subtle; its intensity is enhanced at the N $1s \rightarrow 3s\sigma$ excitation and maybe weakly disturbed around the N $1s \rightarrow 3p\pi$ excitation. The latter could also be due to the N $1s \rightarrow 3p\sigma$ excitation that is located underneath the N $1s \rightarrow 3p\pi$ excitation [16]. The partial ionization cross sections show Fano-like profiles

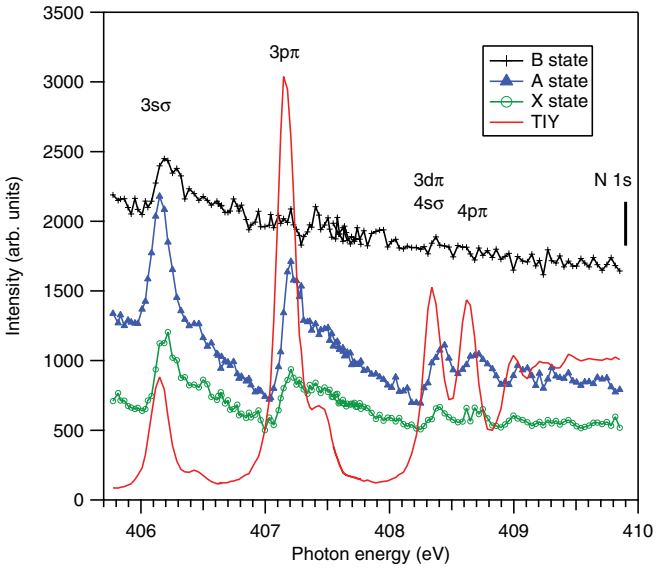

FIG. 3. (Color online) Photoionization intensities of the X, A, and B states in the photon energy region covering the N $1s \rightarrow$ Rydberg excitations up to the N $1s$ edge. The total ion yield (TIY) measured during the photoelectron spectra is shown for comparison.

around the resonances, which is an indication of interference between direct and resonant ionization channels.

The photoionization cross section of the A state was simulated by calculating the total intensity distribution according to Eq. (1) at different photon energies ω and by integrating the total intensity in the spectrum. The result is shown in Fig. 4. The N $1s \rightarrow 3s\sigma$ and $3p\pi$ excitations were calculated separately and the results were added together to get the cross section over the two resonances. Direct photoionization has been included only once in the total intensity. It was assumed to decrease linearly as a function of photon energy, as given

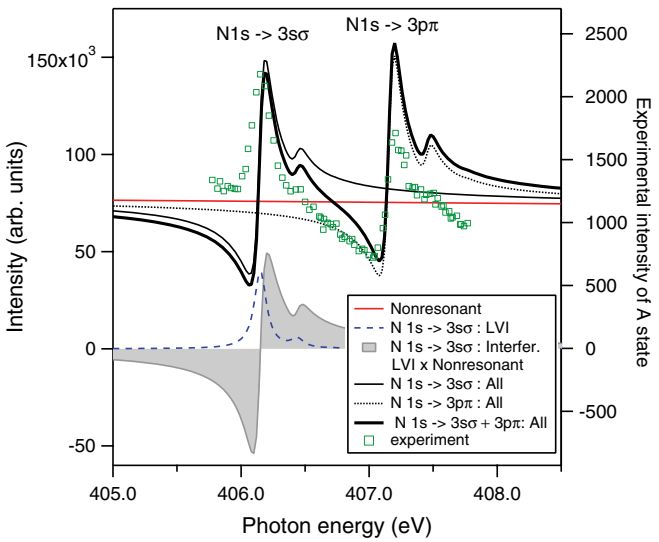

FIG. 4. (Color online) Simulated partial ionization cross section to the $A\ 1\pi_u^{-1}$ state of N_2^+ (thick black curve), assuming the case of two isolated Rydberg resonances N $1s \rightarrow 3s\sigma$ and N $1s \rightarrow 3p\pi$. The partial contributions are shown for the N $1s \rightarrow 3s\sigma$ resonance. Experimental results from Fig. 3 are shown with open squares.

by the asymptotic curve in Fig. 6 of Ref. [12]. The average value for the D:M ratio was ∼23, which reproduced the vibrational intensity distributions in the simulations shown in Fig. 2. The simulated curve reproduces the main features of the experimental relative photoionization cross section of the A state, which is also included in Fig. 4. However, the Fano line shape resulting from the simulation drops too low just before the N $1s \rightarrow 3s\sigma$ excitation and the $\upsilon = 1$ vibrational levels appear too pronounced in the simulated cross section. The drop in the photoionization cross section is due to destructive interference between direct and resonant photoionization, as can be seen from the partial contributions to the cross section that have been plotted for the N $1s \rightarrow 3s\sigma$ excitation. Note that these different contributions were obtained from the simulation at the same time and their intensities were not adjusted afterwards. The contribution due to the interference between direct and resonant photoionization has a maximum at a slightly higher energy than the nominal resonance energy, which is a well-known property of Fano-type interferences. This is predicted to lead to a shift of about 40 meV in the maximum of photoionization cross section (sum of all contributions) of the A state. In the experiment, the maxima of the partial photoionization cross sections in Fig. 3 appear indeed slightly shifted to higher energy than those of the total ion yield spectrum that was measured simultaneously. Note also that the influence of the interference between direct and resonant photoionization extends much further than that of LVI alone.

There are a few possible reasons for the discrepancy between the experimental and calculated partial ionization cross section in Fig. 4. First, interference between different electronic states (N $1s^{-1}3s\sigma^1$ and N $1s^{-1}3p\pi^1$) has not been taken into account in the simulation. Its contribution should, however, be negligible, as the resonances are much further away from each other than their lifetime widths. Second, the N $1s \rightarrow \pi^*$ resonance may still influence the photoelectron intensity of the A state at the energies of core-to-Rydberg excitations, which is in fact implied by the experimental results of Ref. [12]. Third, the electronic transition moment M for the participator decay may depend on the part of the potential energy curve accessed in photoabsorption. Obviously, if M decreased faster than the photoabsorption cross section upon detuning the excitation energy away from the resonant maximum, interference between direct and resonant channels would be weaker before the resonances and destructive interference would also be weaker. This would make the minima less conspicuous than in Fig. 4. The dependence of M on the internuclear distance has been suggested to be important for participator decay to the B state at the N $1s \rightarrow \pi^*$ resonance of N_2 [18].

A detailed discussion of the absolute intensities of resonant Auger transitions is beyond the scope of the present paper. However, we can make several observations of participator decay from the N $1s^{-1}3s\sigma^1$ and N $1s^{-1}3p\pi^1$ states in comparison to the N $1s \rightarrow \pi^*$ resonant spectrum. The latter spectrum shows the most intense transitions to the A state, followed by transitions to the X state, while decay to the B state is extremely weak [2,18]. The participator decay of the N $1s^{-1}3p\pi^1$ state displays similar trends for the intensities of the participator transitions, which is perhaps expected because the symmetry of the excited orbital is π in both cases. In the case of participator decay from the N $1s^{-1}3s\sigma^1$ state, which involves a Rydberg orbital of σ symmetry, the B state gains some intensity, even though it is still less than the A and X states (Fig. 3). As compared to the photoabsorption cross section, the participator decay is strongest at the N $1s \rightarrow 3s\sigma$ excitation among all Rydberg resonances.

V. CONCLUSION

In conclusion, valence photoionization of the N_2 molecule is clearly affected by participator decay from core-to-Rydberg excited states. The effect is observed as Fano line shapes in the relative partial ionization cross sections to the X and A states of the N_2^+ ion and as changes in the vibrational intensities in the photoelectron spectra. These effects can be simulated numerically quite well by taking into account the contributions from LVI, direct photoionization, and interference between direct and resonant photoionization channels.

ACKNOWLEDGMENTS

We thank D. Benedetti (Consiglio Nazionale delle Ricerche, Istituto Officina dei Materiali) and C. Leghissa (Sincrotrone Trieste) for technical assistance prior to the experiments. The research leading to these results has received funding from the European Community Seventh Framework Programme under Grant No. 226716.

[1] W. Eberhardt, J. Stöhr, J. Feldhaus, E. W. Plummer, and F. Sette, Phys. Rev. Lett. **51**, 2370 (1983).

[2] J.-E. Rubensson, M. Neeb, M. Biermann, Z. Xu, and W. Eberhardt, J. Chem. Phys. **99**, 1633 (1993).

[3] R. Fink, J. Electron Spectrosc. Relat. Phenom. **76**, 295 (1995).

[4] M. N. Piancastelli, A. Kivimäki, B. Kempgens, M. Neeb, K. Maier, U. Hergenhahn, A. Rüdel, and A. M. Bradshaw, J. Electron Spectrosc. Relat. Phenom. **98-99**, 111 (1999).

[5] R. Feifel *et al.*, Phys. Rev. A **69**, 022707 (2004).

[6] K. C. Prince, M. Vondráček, J. Karvonen, M. Coreno, R. Camilloni, L. Avaldi, and M. de Simone, J. Electron Spectrosc. Relat. Phenom. **101-103**, 141 (1999).

[7] K. P. Huber and G. Herzberg, *Constants of Diatomic Molecules, Molecular Spectra and Molecular Structure Vol. IV* (Van Nostrand Reinhold, New York, 1979).

[8] V. Carravetta, F. Kh. Gel'mukhanov, H. Ågren, S. Sundin, S. J. Osborne, A. Naves de Brito, O. Björneholm, A. Ausmees, and S. Svensson, Phys. Rev. A **56**, 4665 (1997).

[9] T. Tanaka, H. Shindo, C. Makochekanwa, M. Kitajima, H. Tanaka, A. De Fanis, Y. Tamenori, K. Okada, R. Feifel, S. Sorensen, E. Kukk, and K. Ueda, Phys. Rev. A **72**, 022507 (2005).

[10] W. Eberhardt, J.-E. Rubensson, K. J. Randall, J. Feldhaus, A. L. D. Kilcoyne, A. M. Bradshaw, Z. Xu, and P. D. Johnson, Phys. Scr. **T41**, 143 (1992).

[11] E. Shigemasa, T. Kaneyasu, T. Matsushita, Y. Tamenori, and Y. Hikosaka, New J. Phys. **12**, 063030 (2010).
[12] O. Kugeler, E. E. Rennie, A. Rüdel, M. Meyer, A. Marquette, and U. Hergenhahn, J. Phys. B **37**, 1353 (2004).
[13] K. C. Prince *et al*., J. Synch. Rad. **5**, 565 (1998).
[14] http://wavemetrics.com/.
[15] J. M. Dyke (private communication). For application of the original program see, e.g., L. Golob, N. Jonathan, A. Morris, M. Okuda, K. J. Ross, and D. J. Smith, J. Chem. Soc. Faraday Trans. 2 **71**, 2026 (1975).
[16] J. Adachi, N. Kosugi, and A. Yagishita, J. Phys. B **38**, R127 (2005).
[17] C. T. Chen, Y. Ma, and F. Sette, Phys. Rev. A **40**, 6737 (1989).
[18] M. N. Piancastelli *et al*., J. Phys. B **33**, 1819 (2000).